

Transformation hardening of medium-carbon steel with a fiber laser: the influence of laser power and laser power density

F. Qiu*, V. Kujanpää**

*Laser Processing Laboratory, LUT Metals, Lappeenranta University of Technology, Tuotantokatu 2, 53850 Lappeenranta, Finland, E-mail: feng.qiu@lut.fi

**Laser Processing Laboratory, LUT Metals, Lappeenranta University of Technology, Tuotantokatu 2, 53850 Lappeenranta, Finland, E-mail: veli.kujanpaa@lut.fi

crossref <http://dx.doi.org/10.5755/j01.mech.17.3.510>

1. Introduction

Laser surface treatment is a process of altering the metallurgical and mechanical properties of the material surface with laser irradiation. It is mostly used to produce hard, wear-resistant regions on the workpiece while retaining the bulk material unaffected [1-3]. A defocused laser beam is usually used to heat up the material surface above its austenitization temperature, allowing formation of austenite.

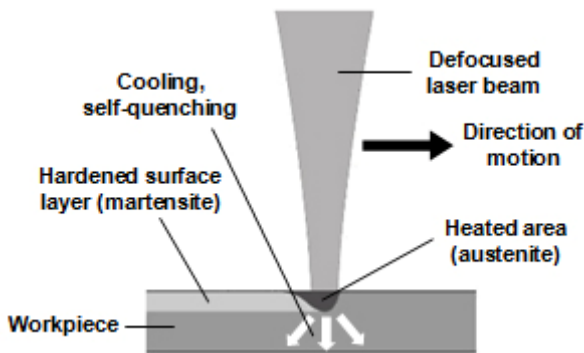


Fig. 1 Basic principle of laser transformation hardening

The base material surrounding the laser irradiated area acts as a heat sink, causing quick self-quenching and phase transformation to martensite [1, 2]. This process is illustrated in Fig. 1.

In recent years, fiber laser systems have been quickly developed for advanced processes [4-7]. Compared with Nd:YAG lasers which are used for industrial purposes, fiber lasers feature simplicity, high electrical-to-optical efficiency, high reliability and relatively low cost of operation [8, 9]. Fiber laser is expected to be suitable for surface hardening of carbon steels, because the wavelength

of radiation produced by laser diodes can be efficiently absorbed by iron-based materials [10]. Although laser transformation hardening is a well-known process, information about laser hardening with fiber laser is basically unavailable.

This study focuses on how the laser power and power density of a fiber laser affect laser hardening of medium-carbon steel samples in the hardness profile across the irradiated track, along the depth below the treated surface and in microstructures. Experimental results are also compared with a previous study by high power diode laser hardening.

2. Experimental procedures

This study uses a work cell containing a CNC XY table and a YLR-5000-S fiber laser equipment which produces a laser beam with a wavelength of 1070-1080 nm and a maximum nominal output power of 5 kW. No shielding gas is used.

The hardening tests are done on two types of medium carbon steels with the same carbon content and different initial microstructures and alloying contents shown in Table 1. Imamic (X15) steel is an as-rolled high-silicon steel featuring higher fatigue strength than conventional microalloy steels. The initial microstructure contains ferrite and pearlite. Uddeholm Impax Supreme (AC16) is a pre-hardened mould steel with high contents of chromium, nickel and molybdenum, in which tempered martensite is the basic initial composite due to quenching and tempering treatment. Comparison of X15 and AC16 samples redounds to reveal how laser power density affects the hardening of medium-carbon steels with various initial microstructures and alloying contents. The surface roughness of all samples, R_a , is about 2.5 μm .

Table 1

Sample used in the hardening test (compositions in weight percentage)

Code	Trademark	Delivered Condition	Initial HV5	Compositions (wt. %)							
				C	Si	Mn	Cr	Ni	Mo	V	Cu
X15	Imamic	As rolled	289	0.375	1.319	0.983	0.163	0.111	0.020	0.110	0.243
AC16	Uddeholm Impax Supreme	Q&T	336	0.373	0.366	1.470	1.860	1.172	0.201	0.006	0.181

The laser power P and the laser power density I_p used in this study are indicated in Table 2. The laser spot size R_s is changed by altering the distance off the focus z and thus I_p is changed. The experiment uses a focusing lens

with the focal length of 150 mm. An output fiber core diameter of 150 μm in the fiber laser is used for the tests on X15 samples. For AC16 samples, an output fiber core diameter of 200 μm is used. The angle between the optical

axis and the surface is 90 degrees. All the tests are done with a constant traverse rate of 8.0 mm/s. The samples are air-cooled after the process.

For X15 steel, the hardened depth is defined as

the distance below the sample's surface where martensite content drops to 50 wt.% of the local microstructures. For AC 16 samples, the hardened depth is defined as the depth where the hardness value reduces to 500 HV.

Table 2

Laser power and laser power density used in the experiments

Test no.	Laser power P , W	Laser power density, I_p , W/cm ² / R_s , Laser spot diameter, mm			
		A	B	C	D
X15_1	955	7224/4.1	8282/3.8	9590/3.6	11231/3.3
X15_2	1423	7496/4.9	8397/4.6	9471/4.4	10765/4.1
X15_3	1900	6145/6.3	6714/6.0	7365/5.7	8117/5.5
X15_4	2840	5065/8.4	5786/7.9	6672/7.4	7779/6.8
X15_5	3788	5012/9.8	5618/9.3	6341/8.7	7212/8.2
AC16_1	944	10955/3.3	12977/3.0	15607/2.8	19112/2.5
AC16_2	1409	12092/3.9	13983/3.6	16351/3.3	*19369/3.0
AC16_3	1883	12425/4.4	14110/4.1	*16159/3.9	*18687/3.6
AC16_4	2816	11952/5.5	13230/5.2	*14724/4.9	*16485/4.7
AC16_5	3750	11083/6.6	12061/6.3	*13174/6.0	*14448/5.7

* Melting is observed on the surface of the irradiated track

3. Results and discussion

3.1. Ferritic-pearlitic steel X15

Fig. 2 shows the surface hardness of X15 workpiece produced by different laser power levels and laser power densities. Under each laser power there is an optimal laser power density which produces the peak hardness. Increase or decrease of laser power density from this optimal point reduces the surface hardness. The peak of the curve shifts to the left as the laser power increases and thus indicates that lower power density is required to produce high hardness with more laser power input. Fig. 3 indicates under each laser power level the optimal laser spot size and the corresponding area that produce the maximum hardness. The optimal spot size is approximately of linear dependence on the laser power, meaning that increase of laser power can significantly increase the hardenable area on the workpiece. The largest measured HV5 value (781) is achieved with the laser power density of 8397 W/cm² under 1423 W laser power.

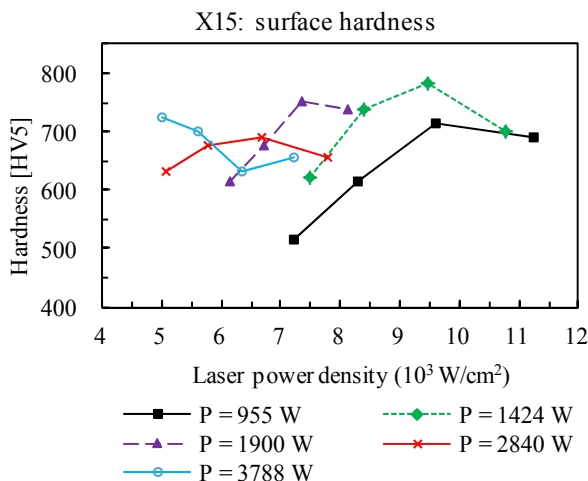


Fig. 2 Surface hardness of X15 samples under various laser power and laser power density

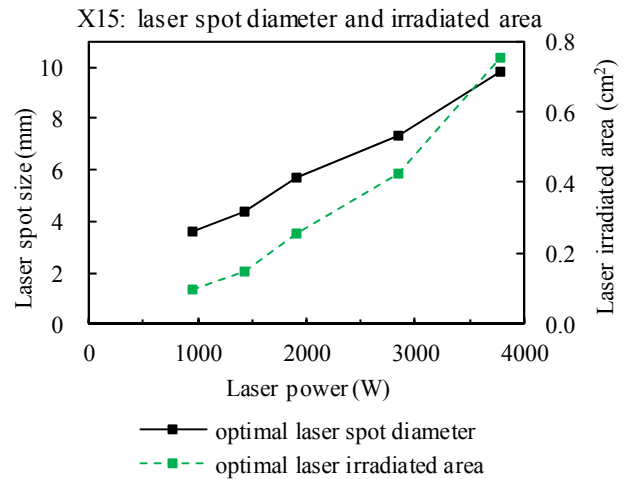


Fig. 3 Optimal laser spot size and laser irradiated area of X15 workpiece under each laser power

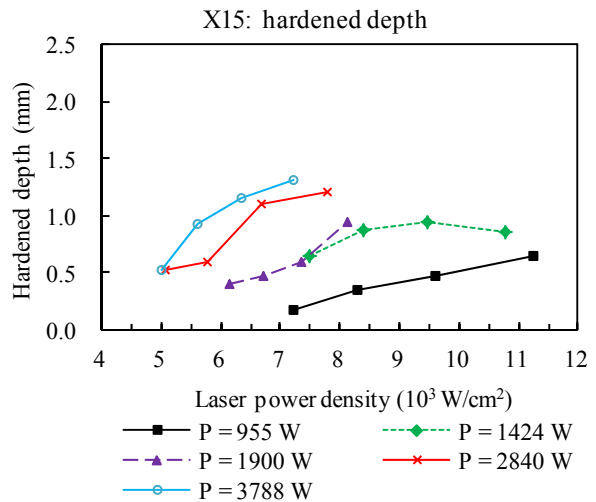


Fig. 4 Hardened depth of X15 samples under various laser power and laser power density

As shown in Fig. 4, increasing the laser power is the basic method of obtaining a deeper hardened layer. However, Fig. 4 also indicates that larger hardened depth can as well be acquired with higher laser power density while retaining the same laser power. This can be done by using a smaller laser spot. The maximum hardened depth of approximately 1.32 mm is produced with 7212 W/cm² laser power density under 3788 W laser power.

These can be explained with the thermal cycle during the laser irradiation. As higher laser power is used, the laser spot size is enlarged by increasing the distance off the focus. As the traverse rate remains constant, the magnified laser irradiated area causes a longer thermal cycle in case that appropriate laser power density is applied. The laser power density required to achieve optimal hardening results is thus reduced. Moreover, as Fig. 2 shows, excessive laser power density lowers the cooling rate and thus

decreases the produced surface hardness.

Fig. 5 shows an example which compares the effects of 7496 W/cm² and 8397 W/cm² power density under 1423 W laser power. It indicates that increase of power density from 7496 W/cm² to 8397 W/cm² facilitates the homogenization of the irradiated area and produces a more homogenous layer of martensite. When the surface of the sample is heated up above its austenitization temperature A_{c1} , the initial crystal structures containing ferrite and pearlite starts to transform to austenite. Carbon diffuses from carbides to ferrite and homogenizes the austenitized area. The hardening effect is determined by the extent of homogenization which relies on the duration the temperature is above A_{c1} and the cooling rate. As all the tests in this study are done with a constant traverse rate, the laser power density is the primary parameter that affect the thermal cycle.

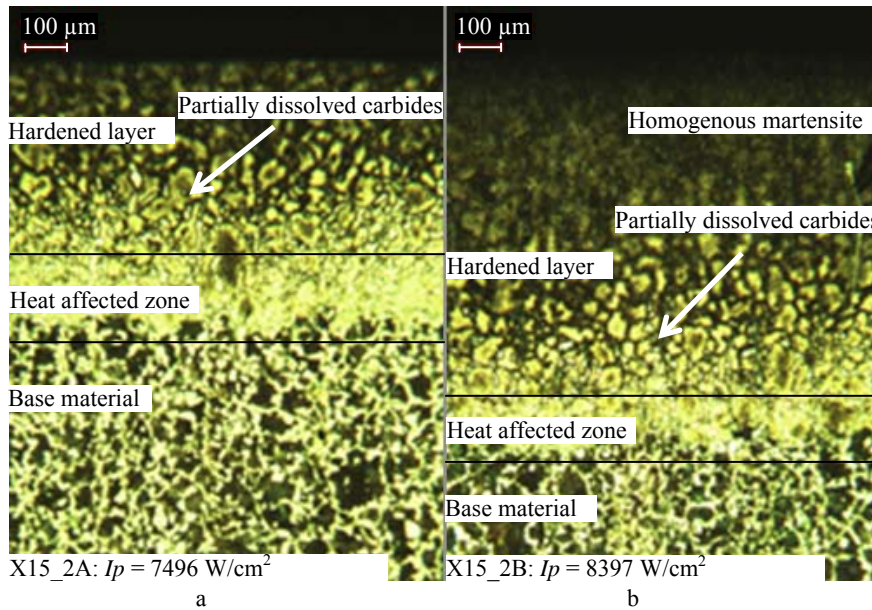


Fig. 5 Microscopic view of cross sections of X15 samples hardened with (a) 7496 W/cm² and (b) 8397 W/cm² laser power density under 1423 W laser power

3.2. Quenched and tempered steel AC16

Fig. 6 shows the surface hardness obtained on AC16 samples with various laser power and laser power density. Similar to Fig. 2, with each laser power there is a

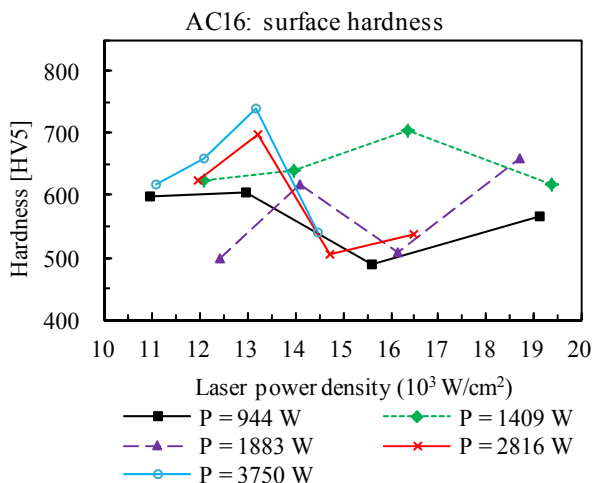


Fig. 6 Surface hardness of AC16 samples under various laser power and laser power density

laser power density producing the maximum hardness. Except for 944 W results, increase of laser power causes the optimal power density to shift leftward and accordingly reduces the laser power density required to produce high

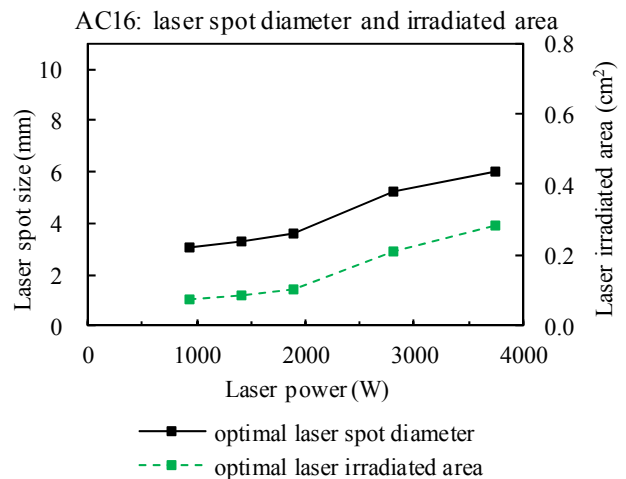


Fig. 7 Optimal laser spot size and laser irradiated area of AC16 workpiece under each laser power

hardness. Fig. 7 shows the dependence of the optimal laser spot size and the irradiated area on laser power. In contrast to Fig. 3, the increase of laser power does not markedly magnify the optimal hardening area on the AC16 workpiece. The hardened depths of AC16 samples are presented in Fig. 8. Increase of laser power results in deeper hardened layer. Increase of laser power density via redu-

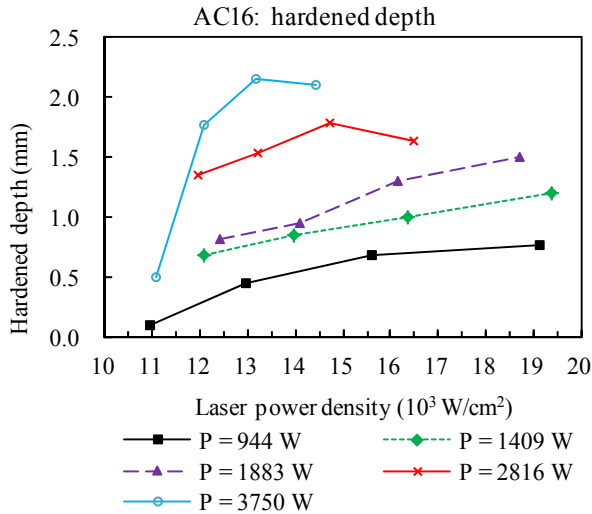


Fig. 8 Hardened depth of X15 samples under various laser power and laser power density

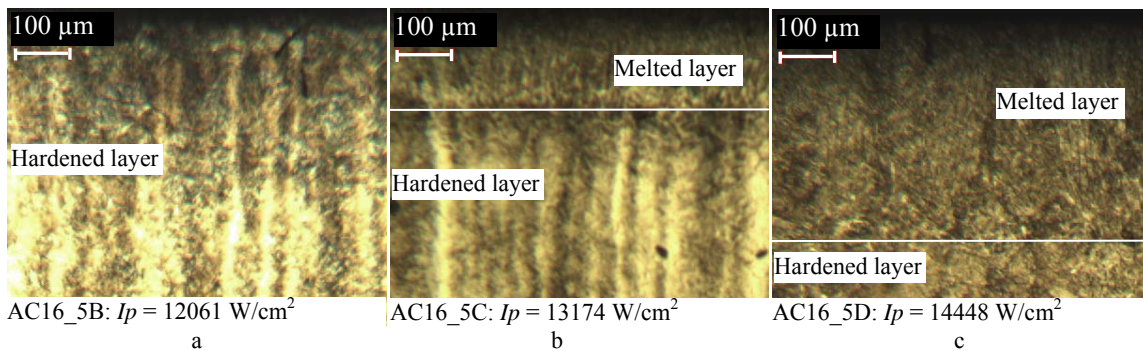


Fig. 9 A microscopic view of the cross sections of AC16 samples hardened with (a) 12061 W/cm^2 , (b) 13174 W/cm^2 and (c) 14448 W/cm^2 laser power density under 3750 W laser power

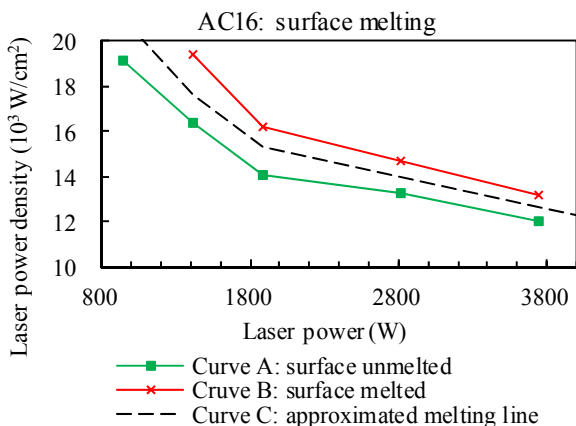


Fig. 10 Surface melting in AC16 tests under various laser power and laser power density

As shown in Fig. 10, curve A and curve B respectively represent non-surface-melting and surface-melting results. A curve C is approximated from experimental data to exhibit the melting condition. Combinations of laser

power and laser power density below curve C result in normal surface hardening and above curve C the risk of surface melting should be taken into consideration.

3.2.1. Surface melting

Surface melting occurs on some of the tests denoted in Table 2. Fig. 6 and Fig. 8 exhibit that surface melting mostly causes dramatic decrease in the surface hardness. However, the results denote that surface melting in some cases may benefit the hardening process. Fig. 9 compares the micrographs of melted and unmelted AC16 samples hardened with 3750 W laser power. Melting occurs on sample 5C and 5D. As indicated in Fig. 6, compared with sample 5B, 5C produces higher surface hardness while 5D shows the opposite. Melting that occurs on 5C does not reduce the surface hardness and may even benefit the hardening result. The thin melted layer shown in Fig. 9 may avail the homogenization of carbon and other elements and is supposed to experience a sufficiently high cooling rate to form homogenous martensite on the sample's surface. In contrast, a much thicker melted layer is produced on sample 5D, which can markedly lower the cooling rate, anneal the sample's surface and hence dramatically reduce the surface hardness.

power and laser power density below curve C result in normal surface hardening and above curve C the risk of surface melting should be taken into consideration.

3.3. Comparison of ferritic-pearlitic steel with quenched and tempered steel

The highest surface hardness values produced on X15 and AC16 samples in the test are both about 780 (HV5). This is basically due to the equal carbon content as shown in Table 1. The carbon content determines the hardness of martensite that can be produced on the material surface and thus the maximum surface hardness obtained on X15 and AC16 samples are close.

Comparing Fig. 4 and Fig. 8, AC16 samples require higher laser power density to achieve the same hardness level as X15. The hardened depth acquired in AC16 samples is relatively high due to the alloy content of Mn, Cr and Ni. Alloy elements decrease the transformation rate of austenite to ferrite and ferrite carbides and make it possible to form martensite with lower cooling rates [11]. This is beneficial to produce a deeper hardened layer.

3.4. Comparison of fiber laser hardening with diode laser hardening

The same samples of the ferritic-pearlitic steel X15 and quenched and tempered steel AC16 were tested in a previous study by Pantsar using a high power diode laser which delivered radiation at wavelengths of 800 ± 10 nm and 940 ± 10 nm [12]. Due to efficient energy absorption by iron-based materials, high power diode laser is considered to be more suitable for hardening steels than other laser types [2]. The tests results are compared with fiber laser hardening in this study as shown in Table 3.

The comparison shows some advantages over high power diode laser. The high power diode laser can produce approximately the same surface hardness in a larger irradiated area with lower laser power. The hardened depth, on the other hand, cannot be compared since the test

data with high power diode laser is not available.

Fiber laser is capable to produce equivalent or even higher surface hardness in hardening of medium-carbon steels. It can be used as an effective tool to achieve both high surface hardness and considerable hardened depth for surface hardening but requires relatively high laser power density which also means smaller irradiated area.

The comparison is however incomplete and inconclusive, since different optics are used and create different laser beam profiles which probably have significant influence on the hardening results. Besides, previous study suggested that change of traverse rate has large effect on the hardening effects [13]. Therefore the optimization of the traverse rate in combination with laser power, laser power density and irradiate area is well worth further investigation.

Table 3

Comparison of fiber laser hardening of steels X15 and AC16 with diode laser hardening in a previous study [12]

Material	Surf. roughness, R_a , μm	Laser	Traverse rate, mm/s	Laser power, W	Irradiated area, cm^2	Laser power density, W/cm^2	HV5	Hardened depth, mm
X15	0.2-0.4	diode laser	10.5	1170	0.65 (rectangle)	1800	743	NA
X15	2.5	fiber laser	8.0	1423	0.17 (circular)	8397	781	1.5
AC16	0.2-0.4	diode laser	10.5	1170	0.65 (rectangle)	1800	772	NA
AC16	2.5	fiber laser	8.0	3750	0.28 (circular)	13174	781	2.25

4. Conclusions

This study investigates how the laser power density of a fiber laser affects the surface transformation hardening of medium-carbon steels. The tests use two materials with different initial microstructures, including X15 which is composed of ferrite and pearlite and AC16 that contains tempered martensite.

The tests on X15 and AC16 samples indicate that under each laser power there is an optimum power density what can produce the maximum hardness. With higher laser power, lower power density is required to produce high hardness. This also means that increase of laser power can markedly enlarge the area that can be hardened. This shows much higher effect on X15 than on AC16. Increase of hardened depth can be either achieved by using higher laser power or by reducing the laser spot size while retaining the laser power unchanged.

Surface melting generally reduces much the surface hardness. But slight surface melting in some exceptional cases may improve the hardening effect.

AC16 requires higher laser power density to achieve the same hardness as X15. Due to the equivalent carbon contents of X15 and AC16, the maximum surface hardness (HV5) obtained on the two materials are both around 781. The hardened depth acquired in AC16 samples is relatively high due to the alloy contents of Mn, Cr and Ni.

For hardening of medium carbon steels, fiber laser may be capable to produce equivalent surface hardness in a smaller circular area, requiring markedly higher laser power density in comparison with high power diode laser. Fiber laser is a potential tool to produce high surface hard-

ness and high hardened depth for medium-carbon steels. Further study is required in optimization with appropriate optics and/or scanning parameters, e.g. the traverse rate.

References

1. **Steen, W.M.** 2003. Laser Material Processing, 3rd ed. London: Springer-Verlag. 408p.
2. **Ion, J.C.** 2002. Laser transformation hardening, Surface Engineering 1: 14-31.
3. **Jonušas, R.; Kalpokas, J.; Petrikas, R., Žunda, A.** 2004. Investigation of laser surface treatment effect on coating adhesion, Mechanika 5(49): 65-71.
4. **Limpert, J.; Rösera, F.; Schreiber, T.; Manek-Höninger, I.; Salinb, F.; Tünnermann, A.** 2006. Ultrafast high power fiber laser systems, Comptes Rendus Physique 7(2): 187-197.
5. **Baumeister, M.; Dickmann, K.; Hout, T.** 2006. Fiber laser micro-cutting of stainless steel sheets, Applied Physics A: Materials Science & Processing 85: 121-124.
6. **Kawahito, Y.; Terajima, T.; Kimura, H.; Kuroda, T.; Nakata, K.; Katayama, S.; Inoue, A.** 2008. High-power fiber laser welding and its application to metallic glass $\text{Zr}_{55}\text{Al}_{10}\text{Ni}_5\text{Cu}_{30}$, Materials Science and Engineering: B 148(1-3): 105-109.
7. **Kah, P.; Salminen, A.; Martikainen, J.** 2010. The effect of the relative location of laser beam with arc in different hybrid welding processes, Mechanika 3(83): 68-74.
8. **Canning, J.** 2006. Fiber lasers and related technologies, Optics and Lasers in Engineering 44: 647-676.
9. **Aouici, H.; Yaltese, M.A.; Fnides, B.; Mabrouki, T.**

2010. Machinability investigation in hard turning of AISI H11 hot work steel with CBN tool, *Mechanika* 6(86): 71-77.
10. **Ready, J.F.** 1997. *Industrial Application of Lasers*, 2nd ed. London: Academic Press. 599p.
11. Edited by **Ready, J.F.**; **Farson, D.F.**; **Feeleyed, T.** 2001. *LIA Handbook of Laser Materials Processing*. Pineville: Magnolia Publishing Inc. 715p.
12. **Pantsar, H.** 2005. Models for diode laser transformation hardening of steels: [D]. Lappeenranta: Lappeenranta University of Technology. 134p.
13. **Arata, Y.**, **Inoue, K.**, **Maruo, H.**, **Miyamoto, I.** 1986. Application of laser for material processing - Heat flow in laser hardening. *Plasma, Electron & Laser Beam Technology, Development and Use in Materials Processing*. American Society for Metals: 550-567.

F. Qiu, V. Kujanpaa

VIDUTINIO ANGLINGUMO PLIENŲ KIETUMO KEITIMAS PLUOŠTINIAIS LAZERIAIS: LAZERIO GALIOS TANKIO ĮTAKA

Re z i u m ė

Straipsnyje tiriama pluoštinio lazerio galios tankio įtaka dviejų vidutinio anglingumo plienų paviršiaus kietumo kitimui. Išfokusuotas lazerio spindulys, gautas naudojant pluoštinių lazerių sistemą, panaudotas bandinio paviršiui apšvitinti. Bandyams panaudoti du vidutinio anglingumo skirtingos pradinės mikrostruktūros plienai: X15 turintis ferito ir perlito, ir AC16, sudarytas iš atleisto martenito. Plieno X15 bandymai parodė, kad bet kokios galios lazeriui būtinas tam tikras optimalus galios tankis, leidžiantis pasiekti maksimalų plieno kietumą. Didėjant lazerio galiai, tiek reikiamam paviršiaus kietumui, tiek sukietinimo gyliui pasiekti optimalus galios tankis mažėja. Nustatyta, kad plieno AC16 maksimalus kietumas nepriklauso nuo lazerio galios tankio. Legiruojantieji elementai gali padidinti sukietinimo gylį. Nedidelis paviršiaus aplydimas gali palengvinti sukietinimo procesą ir padidinti paviršiaus kietumą. Sukietinimo gylis dažniausiai padidėja padidėjus lazerio galiai ir/arba lazerio galios tankiui. Kaip ir kitų tipų lazeriai, pluoštinis lazeris tinka vidutinio anglingumo plienams sukietinti.

F. Qiu, V. Kujanpää

TRANSFORMATION HARDENING OF MEDIUM-CARBON STEEL WITH A FIBER LASER: THE INFLUENCE OF LASER POWER DENSITY

S u m m a r y

This paper investigates the effects of laser power density of a fiber laser on surface transformation hardening of two types of medium-carbon steels. An out-of-focus laser beam produced by a fiber laser system is used to produce an irradiated track on the surface of the samples. The tests use two types of medium-carbon steels with different initial microstructures, including X15 containing ferrite and pearlite and AC16 composed of tempered martensite. The tests on X15 show that for each laser power there is an

optimum power density that produces the maximum hardness. With increased laser power, the optimal power density for both surface hardness and hardened depth is lowered. For AC16 tests, the maximum hardness value is not found to be dependent on laser power density. Alloying elements may increase the hardened depth. Slight surface melting may facilitate the hardening process and increase the surface hardness. The hardened depth is generally increased with higher laser power and/or laser power density. Compared with other types of lasers, fiber laser is a competitive tool in hardening of medium-carbon steels.

Keywords: fiber laser, hardening, carbon steel, power density, pearlite and ferrite, tempered martensite.

Ф. Киу, И. Куянпaa

ИЗМЕНЕНИЕ ТВЕРДОСТИ ПОВЕРХНОСТИ СРЕДНЕУГЛЕРОДИСТЫХ СТАЛЕЙ ПРИ ПОМОЩИ ВОЛОКОННЫХ ЛАЗЕРОВ: ВЛИЯНИЕ ПЛОТНОСТИ МОЩНОСТИ ЛАЗЕРА

Р е з ю м е

В статье рассматривается влияние плотности мощности волоконного лазера на изменение твердости поверхности двух среднеуглеродистых сталей. Расфокусированный луч лазера, полученный при помощи системы волоконных лазеров, использован для облучения поверхности образца. Для экспериментов использованы две среднеуглеродистые стали с разными исходными микроструктурами: сталь X15 с ферито-перлитной и сталь AC16 с отпущенного мартенсита структурами. Исследования стали X15 показали, что для лазера любой мощности существует оптимальная плотность мощности, обеспечивающая максимальную твердость. При повышении мощности лазера оптимальная плотность мощности как на твердость поверхности, так на глубину упрочнения уменьшается. Определено, что для стали AC16 максимальная твердость не зависит от плотности мощности лазера. Легирующие элементы могут увеличить глубину упрочнения. Наплавка поверхности может облегчить процесс упрочнения и повысить твердость поверхности. Глубина упрочнения чаще всего увеличивается при повышении мощности лазера и/или плотности мощности лазера. По сравнению с другими типами лазеров, волоконный лазер является равноценным инструментом для упрочнения среднеуглеродистых сталей.

Received December 09, 2010

Accepted May 19, 2011